Josephson vortices at tricrystal boundaries

V. G. Kogan and J. R. Clem
Ames Laboratory and Department of Physics and Astronomy, Iowa State University, Ames, Iowa 50011

J. R. Kirtley
IBM Research, PO Box 218, Yorktown Heights, New York 10598

(Received 26 August 1999; revised manuscript received 5 October 1999)

Josephson vortices at tricrystal boundaries with and without a π junction in zero applied field are considered. It is shown that if the three tricrystal arms are conventional junctions, a one-flux-quantum ϕ_0 vortex at or near the intersection has lower energy than one far from the intersection. If the largest Josephson length exceeds the sum of the other two, the tricrystal ceases to be a pinning site. If one of the tricrystal arms is a π junction, a $\phi_0/2$ vortex at the intersection is the ground state of the system, and an even number of $\phi_0/2$ vortices is forbidden, whereas $3\phi_0/2$ and $5\phi_0/2$ correspond to possible but, in general, metastable states. For certain combinations of Josephson lengths, the $3\phi_0/2$ state has lower energy than the combined energy of the $\phi_0/2$ vortex at the tricrystal joint and a ϕ_0 vortex far from the joint. Conditions are discussed under which the $3\phi_0/2$ vortex can be observed.

I. INTRODUCTION

Progress has recently been made in studying Josephson boundaries between anisotropic superconductors in general and for high-T_c materials, in particular. The *d*-wave symmetry of the order parameter in the latter makes the boundaries particularly sensitive to crystalline misorientation. In fact, this sensitivity has been employed in some of the most convincing experiments confirming the d-wave symmetry in several optimally doped cuprate superconductors.[1–3] These experiments have been done on ''tricrystal'' boundaries formed by three YBCO crystals having common *c* axis but misaligned axes a,b.

According to Sigrist and Rice,[4] a leading term in the Josephson critical current through a boundary of misaligned *d*-wave grains is $j_c = j_0 \cos 2\chi_1 \cos 2\chi_2$ with $\chi_{1,2}$ being the angles between the grains' *a* axes and the normal to the boundary. This implies that the Josephson currents through two boundaries with different signs of the product $\cos 2\chi_1 \cos 2\chi_2$ should flow in opposite directions for the same phase differences at the boundaries. Therefore, the distribution of the phase difference at a boundary is described either by

$$\lambda_J^2 \varphi'' = \sin\varphi, \tag{1}$$

or by

$$\lambda_J^2 \varphi'' = -\sin\varphi, \tag{2}$$

depending on the sign of j_c. Here, the Josephson lengths $\lambda_J \propto |j_c|^{-1/2}$ may vary due to differences in the crystals' misalignment and in the quality of the boundaries. The primes denote differentiation with respect to the coordinate u in the boundary plane (u,z), where z is the magnetic field direction. The minus sign in Eq. (2) is often incorporated as an extra phase difference of π (a convention we will not follow in this text).[5] Thus, boundaries described by Eq. (2) are called ''π junctions,'' while those obeying Eq. (1) are ''0'' or conventional junctions.

It is worth noting that boundaries with properties of π junctions are not necessarily related to unconventional superconducting symmetries; magnetic impurities in the junction plane or thin ferromagnetic interlayers may produce similar effects.[5,6]

We provide below static solutions for Josephson vortices at semi-infinite tricrystal boundaries with and without a π arm. Although magnetic imaging experiments[3] were done on tricrystal boundaries between thin film grains grown epitaxially on tricrystal substrates of $SrTiO_3$, our model is for bulk tricrystals infinite in the direction *z* of the vortex field. In fact we solve a one-dimensional problem similar to one for a Josephson vortex at an infinite boundary. We show that vortices at tricrystal boundaries with semi-infinite arms are in fact made of ''pieces'' of Josephson vortices of a single infinite boundary, i.e., of the well known solitonlike solutions of the sine-Gordon equations (1) and (2). We calculate energies for various configurations and show that the tricrystal made of three 0 arms may or may not pin a vortex at the arms' intersection or near it depending on relative values of the arms' Josephson lengths. If one of the arms is π, the tricrystal contains a half-flux-quantum vortex, $\phi_0/2$, in the ground state. The only other possible states are $3\phi_0/2$ and $5\phi_0/2$, which, however, have higher energies.

II. CONVENTIONAL TRICRYSTAL BOUNDARY

Let us turn first to tricrystals with no π junctions. For the sake of simplicity we consider tricrystals with members A,B,C having the same London penetration depth λ_L. Directions of the boundaries 1,2,3, which meet at the origin, are arbitrary; see a sketch in Fig. 1(a). Throughout this text, we consider boundaries with

$$\lambda_J \gg \lambda_L. \tag{3}$$

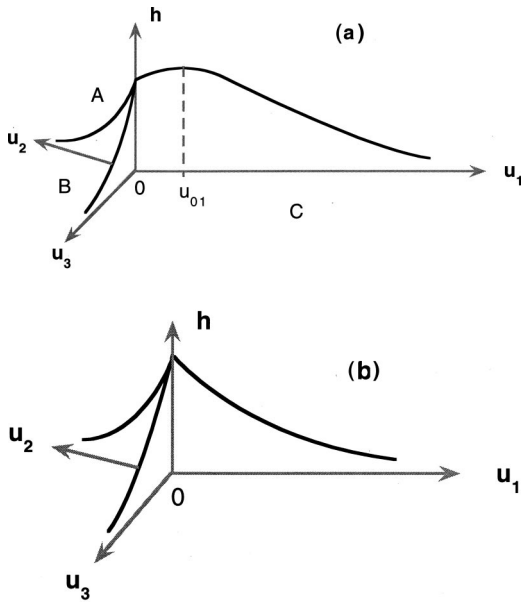

FIG. 1. Field distributions $h(u_{1,2,3})$ at the tricrystal boundaries 1,2,3 are sketched; A,B,C label the three crystals that make up the tricrystal. (a) The distribution for three conventional arms with Josephson lengths satisfying the inequalities: $\lambda_2+\lambda_3>\lambda_1$ and $\lambda_2^2+\lambda_3^2<\lambda_1^2$ [region (a) in Fig. 2]. If one of the arms is a π junction and λ_1 is the largest, this type of distribution corresponds to a total flux of $3\phi_0/2$. (b) The distribution for a 0 tricrystal with $\lambda_2^2+\lambda_3^2>\lambda_1^2$ [region (b) in Fig. 2]. If one of the arms is a π junction, this distribution corresponds to the ground state with a total flux of $\phi_0/2$.

To find the field and phase distributions for a vortex at such a boundary one should solve the sine-Gordon equation (1) for each arm so as to satisfy boundary conditions at infinity and at the tricrystal intersection.

Thus, for the ith boundary we have $\lambda_i^2\varphi_i''=\sin\varphi_i$ where the subscript J of Josephson lengths is omitted for brevity. The prime denotes differentiation with respect to the coordinate u_i along the ith boundary measured from the intersection. One follows the standard procedure: multiply Eq. (1) by φ_i' to get the first integral $\lambda_i^2\varphi_i'^2/2=C_i-\cos\varphi_i$. The Josephson current and the field at the junction ($\propto\varphi_i'$) should vanish as $u_i\to\infty$; this yields $C_i=1$ for $\varphi_i(\infty)=2\pi$. We then obtain

$$\varphi_i=4\tan^{-1}(e^{(u_i-u_{i0})/\lambda_J})+2\pi n_i, \tag{4}$$

where the n_i are integers. The arbitrary constants u_{i0} and n_i are to be fixed by boundary conditions.

The field at the junction planes:[7,8]

$$h_z(u_i)=\frac{\phi_0}{4\pi\lambda_L}\frac{d\varphi_i}{du_i}=\frac{\phi_0}{2\pi\lambda_L\lambda_i}\mathrm{sech}\frac{u_i-u_{0i}}{\lambda_i} \tag{5}$$

(the thickness of the insulated layer is assumed small relative to λ_L). It is worth noting that $d\varphi_i/du_i$ is positive everywhere, corresponding to the field having the same direction everywhere in the junction.

Clearly, one reaches the same value of the field at the origin no matter along which of the boundaries the origin is approached. Equation (5) then gives two equations for the three unknown u_{0i}'s:

$$\lambda_1\cosh\frac{u_{01}}{\lambda_1}=\lambda_2\cosh\frac{u_{02}}{\lambda_2}=\lambda_3\cosh\frac{u_{03}}{\lambda_3}. \tag{6}$$

Another condition is provided by flux quantization: for a standard vortex sitting near the origin, the gauge invariant phase φ changes by 2π if one circles the origin at large distances where the phase, in fact, changes only at the junctions: $\Sigma_i\varphi_i(\infty)=2\pi$. Equation (4) gives $\varphi_i(\infty)=2\pi(n_i+1)$, and therefore $\Sigma_i n_i=-2$. We can choose the n_i's as $(0,-1,-1)$. Then the solutions for the three boundaries are

$$\begin{aligned}\varphi_1&=4\tan^{-1}(e^{(u_1-u_{10})/\lambda_1}),\\ \varphi_2&=4\tan^{-1}(e^{(u_2-u_{20})/\lambda_2})-2\pi,\\ \varphi_3&=4\tan^{-1}(e^{(u_3-u_{30})/\lambda_3})-2\pi.\end{aligned} \tag{7}$$

The field distribution at the junction does not depend on the choice of integers n_i.

We now circle the origin along an infinitesimally small contour. Since the magnetic flux through such a contour is zero, the total change of the gauge-invariant phase difference vanishes. Indeed, denoting by θ_{Ai} the phase at the side A of the ith boundary [see Fig. 1(a)] we have

$$\sum_i\varphi_i=(\theta_{A1}-\theta_{C1})+(\theta_{B2}-\theta_{A2})+(\theta_{C3}-\theta_{B3})\to 0, \tag{8}$$

because $\theta_{A1}\to\theta_{A2}$, $\theta_{B2}\to\theta_{B3}$, and $\theta_{C3}\to\theta_{C1}$. As the circle shrinks, θ_{A1} and θ_{A2} belong to merging points of the same superconductor; the same is true for the two other pairs of θ's.

Setting $u_i=0$ in Eqs. (7) at the intersection, we obtain from Eq. (8)

$$\sum\alpha_i=\pi,\quad \alpha_i=\tan^{-1}(e^{-u_{0i}/\lambda_i}). \tag{9}$$

This completes the system of Eqs. (6) for u_{0i}. To solve this system, we note that in terms of α_i,

$$\cosh(u_{0i}/\lambda_i)=1/\sin 2\alpha_i, \tag{10}$$

and the system (6) and (9) transforms to

$$\lambda_2\sin 2\alpha_1=\lambda_1\sin 2\alpha_2, \tag{11}$$

$$\lambda_3\sin 2\alpha_1=\lambda_1\sin 2\alpha_3, \tag{12}$$

$$\alpha_3=\pi-\alpha_1-\alpha_2. \tag{13}$$

If λ_1 is the largest of the three, it is convenient to introduce the ratios $\gamma_2=\lambda_2/\lambda_1<1$ and $\gamma_3=\lambda_3/\lambda_1<1$. In terms of these ratios the solutions read

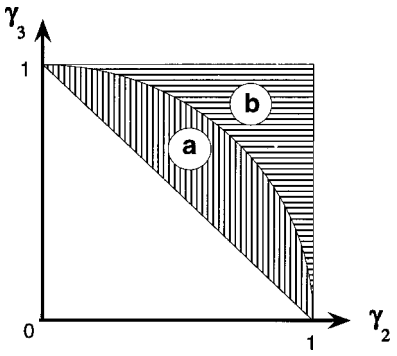

FIG. 2. Domains of the plane $\gamma_2=\lambda_2/\lambda_1, \gamma_3=\lambda_3/\lambda_1$ in which the field distributions (a) and (b) of Fig. 1 are realized for tricrystals with three 0 arms.

$$\cos 2\alpha_1=\frac{1-\gamma_2^2-\gamma_3^2}{2\gamma_2\gamma_3},$$

$$\cos 2\alpha_2=\frac{\gamma_2^2-\gamma_3^2-1}{2\gamma_3}, \tag{14}$$

$$\cos 2\alpha_3=\frac{\gamma_3^2-\gamma_2^2-1}{2\gamma_2}.$$

A straightforward calculation now gives

$$u_{01}=\frac{\lambda_1}{2}\ln\frac{1-(\gamma_2-\gamma_3)^2}{(\gamma_2+\gamma_3)^2-1}, \tag{15}$$

$$u_{02}=\frac{\lambda_2}{2}\ln\frac{\gamma_2-(\gamma_3-1)^2}{(\gamma_3+1)^2-\gamma_2}, \tag{16}$$

$$u_{03}=\frac{\lambda_3}{2}\ln\frac{\gamma_3^2-(\gamma_2-1)^2}{(\gamma_2+1)^2-\gamma_3^2}. \tag{17}$$

Equation (15) shows that these solutions exist provided $\gamma_2+\gamma_3>1$ or

$$\lambda_1<\lambda_2+\lambda_3. \tag{18}$$

This restriction implies that the vortex cannot exist at the tricrystal intersection if the critical current at one of the boundaries is too small relative to the two others.

Figure 2 shows the domain of possible γ's as the shaded area in the upper-right half of the square $0<\gamma_{2,3}<1$ where the condition (18) is satisfied. The line $\gamma_2^2+\gamma_3^2=1$ separates domain (a) of positive u_{01} from the domain (b) where $u_{01}<0$. These boundaries are obtained by examining the argument of ln in Eq. (15). Similar analysis of Eqs. (16) and (17) shows that both u_{02} and u_{03} are negative in the shaded area of possible γ's. The field distribution at the junction are obtained with the help of Eqs. (5) and of now known constants u_{0i}. Sketches of field distributions at the junction corresponding to the domains (a) and (b) are shown in Figs. 1(a) and 1(b). The field maximum is not necessarily at the junction intersection; for γ's in the domain (a), the field maximum is at the arm with largest λ_J and moves away from the intersection as the γ's move from the line $\gamma_2^2+\gamma_3^2=1$ to the boundary of the allowed γ's at the square diagonal $\gamma_2+\gamma_3=1$.

For $\lambda_1=\lambda_2=\lambda_3$, one has $\alpha_i=\pi/3$ and $u_{0i}=-\lambda_J\ln\sqrt{3}<0$. The field distribution is of the form shown in Fig. 1(b). The maximum field value reached at the origin is

$$h(0)=\frac{\phi_0}{2\pi\lambda_L\lambda_J}\sin 2\alpha=\frac{\phi_0}{2\pi\lambda_L\lambda_J}\frac{\sqrt{3}}{2}, \tag{19}$$

i.e., it is about 0.87 of the maximum field for a single boundary Josephson vortex.

The energy per unit length in the z direction of the ith arm reads[7,8]

$$\epsilon_i=\frac{\phi_0^2}{32\pi^3\lambda_L\lambda_i^2}\int_0^\infty du_i\left(1-\cos\varphi_i+\frac{1}{2}(\lambda_i\varphi_i')^2\right)$$

$$=\frac{\phi_0^2}{16\pi^3\lambda_L\lambda_i^2}\int_0^\infty du_i(1-\cos\varphi_i), \tag{20}$$

where the first integral of the sin-Gordon equation has been used. Using solutions (7) we obtain the total energy of the tricrystal boundary after straightforward algebra:

$$\epsilon=\frac{\phi_0^2}{4\pi^3\lambda_L}\sum_{i=1}^{3}\frac{1}{\lambda_i(e^{-2u_{0i}/\lambda_i}+1)}. \tag{21}$$

With the help of the definitions (9) of the α's one can write the exponentials here in terms of the already known $\cos 2\alpha_i$, Eq. (14). Then we obtain

$$\frac{\epsilon}{\epsilon_1}=1-\frac{(1-\gamma_2-\gamma_3)^2}{4\gamma_2\gamma_3}. \tag{22}$$

Here, ϵ_1 is the energy of a Josephson vortex situated far from the intersection at the arm with the largest λ_J; see, e.g., Refs. 7 and 8:

$$\epsilon_1=\frac{\phi_0^2}{4\pi^3\lambda_L\lambda_1}. \tag{23}$$

Thus, for any $\gamma_{2,3}$ in the domain of possible γ's, $\epsilon/\epsilon_1\leqslant 1$. In other words, there is a ''potential well'' for a vortex at the intersection or nearby for any junction parameters obeying restriction (18). The quotation marks are here because, strictly speaking, there are no static solutions except for the vortex sitting at or near the intersection or, alternatively, at distances $u_0\gg\lambda_J$ far from the intersection at any of the arms. Still, solutions of the sine-Gordon equation with time should exist describing vortices moving towards the intersection.

III. ONE OF THE BOUNDARIES IS A π JUNCTION

At the π arm we have to solve Eq. (2). We consider this arm as the first and write the first integral as $\lambda_1^2\varphi_1'^2/2=C_1+\cos\varphi_1$. The Josephson current and the field should vanish as $u_1\to\infty$; this yields $C_1=1$ for $\varphi_i(\infty)=\pi$ (or an odd number of π's; the even possibility is excluded because $C_1+\cos\varphi_1$ must be positive). We then obtain

$$\varphi_1=\pi-4\tan^{-1}(e^{(u_{10}-u_1)/\lambda_1}). \tag{24}$$

Note that for a single boundary infinite in both directions $\varphi_1(\pm\infty)=\pm\pi$, i.e., an isolated vortex at the π boundary carries the flux ϕ_0. For the two 0 arms we have

$$\varphi_2=4\tan^{-1}(e^{(u_2-u_{20})/\lambda_2})-2\pi n_2,$$

$$\varphi_3=4\tan^{-1}(e^{(u_3-u_{30})/\lambda_3})-2\pi n_3. \tag{25}$$

To make solutions $\varphi_{1,2,3}$ more symmetric we rewrite φ_1 utilizing $\tan^{-1}(1/x)=\pi/2-\tan^{-1}x$:

$$\varphi_1=4\tan^{-1}(e^{(u_1-u_{10})/\lambda_1})-\pi. \tag{26}$$

The flux at each of the arms is given by

$$\Phi_i=\frac{\phi_0}{2\pi}[\varphi_i(\infty)-\varphi_i(0)], \tag{27}$$

see Eq. (5) and recall that the junction width is $2\lambda_L$. Since at the origin $\Sigma_i\varphi_i(0)=0$, see Eq. (8), we obtain the total flux Φ through the tricrystal

$$\Phi=\phi_0\sum_i \varphi_i(\infty)/2\pi. \tag{28}$$

With the help of Eqs. (26) and (25) this yields

$$\frac{\Phi}{\phi_0}=\frac{5}{2}-(n_2+n_3). \tag{29}$$

Thus, the flux Φ must be a half-integer of ϕ_0 (an odd number of $\phi_0/2$), a nontrivial result because in the tricrystal with three 0 junctions any integer number of ϕ_0 is permitted. In particular, the tricrystal with one π arm cannot be in a state with $\Phi=0$, the physical situation first discussed in Ref. 5. We write the total flux as

$$\Phi=\frac{\phi_0}{2}(2m+1),\quad m=0,1,2,\ldots, \tag{30}$$

where $n_2+n_3=2-m$.

We now specify the condition $\Sigma_i\varphi_i(0)=0$, the derivation of which does not depend on the junction's type. Using notation (9) for the α's, we obtain

$$\sum_i \alpha_i=\frac{\pi}{4}(5-2m). \tag{31}$$

The next step is similar to that made above: we require that the fields at all arms go to the same limit at the intersection. This gives for α_i the system (11) and (12) and Eq. (31). We exclude α_3 using Eq. (31)

$$\sin 2\alpha_3=(-1)^m\cos 2(\alpha_1+\alpha_2). \tag{32}$$

Further treatment depends on whether m is even or odd.

For m even, $\sin 2\alpha_3=\cos 2(\alpha_1+\alpha_2)$. Introducing new variables $\eta=\sin 2\alpha_1$ and $\gamma_i=\lambda_i/\lambda_1$, we rewrite Eqs. (11) and (12) in a compact form:

$$\sin 2\alpha_i=\gamma_i\eta. \tag{33}$$

Equation (32), which completes the system, reads now as

$$\sqrt{(1-\eta^2)(1-\gamma_2^2\eta^2)}-\gamma_2\eta^2=\gamma_3\eta. \tag{34}$$

Unlike the preceding section, the γ's here may exceed unity if λ_1 is not the largest of the three Josephson lengths. Equation (34) for η can also be written as

$$2\gamma_2\gamma_3\eta^3+(1+\gamma_2^2+\gamma_3^2)\eta^2-1=0. \tag{35}$$

The quantity η is related to the field at the origin

$$h(0)=\frac{\phi_0}{2\pi\lambda_L\lambda_1}\sin 2\alpha_1=\frac{\phi_0}{2\pi\lambda_L\lambda_1}\eta. \tag{36}$$

Given our choice of the field direction, η is positive. Hence, we are looking for a root of Eq. (35) such that $0<\eta<1$.

The cubic polynomial $P(\eta)$ on the left-hand side (LHS) of Eq. (35) has a minimum at $\eta=0$ and a maximum at $\eta=-(1+\gamma_2^2+\gamma_3^2)/3\gamma_2\gamma_3$. Since $P(0)=-1$ and $P(1)=(\gamma_2+\gamma_3)^2>0$, Eq. (35) always has one positive root $\eta<1$.

Consider now the case of an odd m, which changes the sign of the right-hand side (RHS) of Eq. (32). The same treatment as above yields a different equation for η:

$$2\gamma_2\gamma_3\eta^3-(1+\gamma_2^2+\gamma_3^2)\eta^2+1=0. \tag{37}$$

The cubic polynomial $Q(\eta)$ on the LHS of this equation has the following properties: $Q(0)=1$ and $Q(1)=-(\gamma_2-\gamma_3)^2\leqslant 0$. Further, $Q(\eta)$ has a maximum at $\eta=0$ and a minimum at $\eta=(1+\gamma_2^2+\gamma_3^2)/3\gamma_2\gamma_3$. Again, there is always a root $0<\eta<1$.

Let us turn now to the question of energies. For the π arm, the energy functional which generates Eq. (2) reads

$$\epsilon^{(\pi)}=\frac{\phi_0^2}{32\pi^3\lambda_L\lambda_1^2}\int_0^\infty du_1\left(1+\cos\varphi_1+\frac{1}{2}(\lambda_1\varphi_1')^2\right). \tag{38}$$

The energy so defined is proportional to the junction length if the phase difference $\varphi_1\equiv 0$ everywhere. Physically, this means that the zero-current state is not the ground state of a π junction.[5] One, of course, could add a constant to the integrand above to gauge the energy of the zero-current state to zero or any other value; we however find the choice (38) most convenient.[9,10] As with 0 arms, we use the first integral of Eq. (2) to obtain

$$\epsilon^{(\pi)}=\frac{\phi_0^2}{16\pi^3\lambda_L\lambda_1^2}\int_0^\infty du_1(1+\cos\varphi_1). \tag{39}$$

We now employ the solutions (26) and (25) to show that Eq. (21) still holds. One then obtains

$$\frac{\epsilon}{\epsilon_1}=\sum_{i=1}^3\frac{1}{\gamma_i(e^{-2u_{0i}/\lambda_i}+1)}=\frac{1}{2}\sum\frac{e^{u_{0i}/\lambda_i}}{\gamma_i\cosh(u_{0i}/\lambda_i)}$$

$$=\frac{1}{2}\sum\frac{\sin 2\alpha_i}{\gamma_i}e^{u_{0i}/\lambda_i}=\frac{\eta}{2}\sum e^{u_{0i}/\lambda_i}. \tag{40}$$

Here, ϵ_1 is given in Eq. (23) and η is a root of either Eq. (35) or Eq. (37) depending on parity of m. Making the last step in this transformation, we used Eqs. (33).

To express exponentials in Eq. (40) in terms of η we utilize $\gamma_i\eta=\sin 2\alpha_i=1/\cosh(u_{0i}/\lambda_i)$, which yields a quadratic equation for e^{u_{0i}/λ_i} and results in

$$e^{u_{0i}/\lambda_i}=\frac{1\pm\sqrt{1-\gamma_i^2\eta^2}}{\gamma_i\eta}; \tag{41}$$

$\gamma_i\eta=\sin 2\alpha_i<1$, so that this expression is real. The minus sign here corresponds to $u_{0i}<0$, whereas the plus results in $u_{0i}>0$ (substitute $1/\gamma_i\eta=\cosh\mu$ to transform the RHS to $e^{\pm\mu}$). The constants u_{0i} determine the shape of the field distribution because u_{0i} is the position of the field maximum at the ith arm; positive u_{0i} corresponds to $h(u_i)$ sketched on the first arm of Fig. 1(a), while the negative u_{0i} means a monotonic decrease of $h(u_i)$ along the whole arm, as along arms 2 and 3 of this figure. Moreover, since the solutions for the phase at each of the arms are in fact the truncated solitonlike solutions for infinitely long junctions, we conclude that positive u_{0i} correspond to the arm flux $\Phi_i>\phi_0/2$, whereas arms with $u_{0i}<0$ contain $\Phi_i<\phi_0/2$. This conclusion is easily verified using Φ_i of Eq. (27) and the solutions (26) and (25):

$$\Phi_i=\frac{2\phi_0}{\pi}\tan^{-1}(e^{u_{i0}/\lambda_i}). \tag{42}$$

We now obtain for the energy

$$\frac{\epsilon}{\epsilon_1}=\frac{1}{2}\sum_{i=1}^{3}\frac{1\pm\sqrt{1-\gamma_i^2\eta^2}}{\gamma_i}. \tag{43}$$

Note that the energy Eq. (43) and fluxes (42) do not explicitly contain the integer m which determines the total flux Φ. This connection is established implicitly by different choices of signs in Eqs. (41) and (43).

Let us begin with the simplest situation when all λ_J's are the same; i.e., $\gamma_i=1$. Then, for even m, Eq. (35) yields $\eta=1/2$, which results in $\exp(u_{0i}/\lambda_i)=2\pm\sqrt{3}$. For $m=0$ and $\Phi=\phi_0/2$, each $\Phi_i<\phi_0/2$ and all $u_{0i}<0$; therefore, we arrive to the combination of signs $(-,-,-)$ in the sum (43) and to the energy

$$\frac{\epsilon(\phi_0/2)}{\epsilon_1}=\frac{3}{2}\left(1-\sqrt{\frac{3}{2}}\right). \tag{44}$$

The field in the three arms is given by Eqs. (5), which yields

$$h(0)=\frac{\phi_0}{2\pi\lambda_L\lambda_i}\operatorname{sech}\frac{u_{0i}}{\lambda_i} \tag{45}$$

at the intersection. We will not write down cumbersome formulas for $h_i(u_i)$ in terms of material parameters. We note, however, that unless all $u_{0i}=0$ (the case of identical λ_i and $\gamma_i=1$) the field has a cusp at the intersection as in the sketch of Fig. 1(b). The cusp is, of course, smeared over distances of the order λ_L. As expected, Eq. (42) yields the fluxes $\Phi_i=\phi_0/6$.

For $m=2$ and $\Phi=5\phi_0/2$, we can use a similar argument: Each arm may contain a maximum flux of ϕ_0; we do not consider situations with more than one vortex per arm. Then, each one of the three branches must carry flux $\Phi_i>\phi_0/2$.

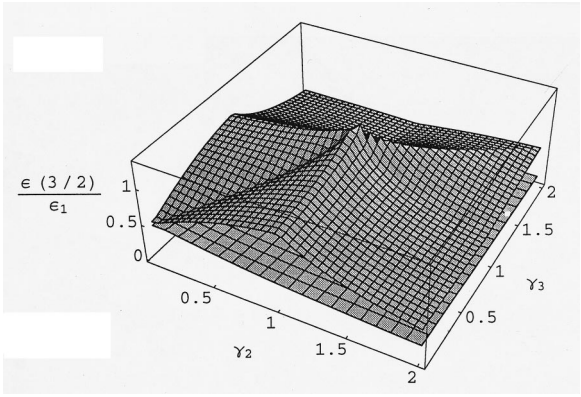

FIG. 3. The energy of the $3\phi_0/2$ vortex as a function of $\gamma_2=\lambda_2/\lambda_1, \gamma_3=\lambda_3/\lambda_1$ in units of $\epsilon_1=\phi_0^2/4\pi^3\lambda_L\lambda_1$, the energy of a ϕ_0 vortex at the π arm with the Josephson length λ_1 far away from the tricrystal intersection. Note a sharp peak at $\gamma_2=\gamma_3=1$ where $\epsilon(1,1)/\epsilon_1=1.5$. The energy of the $\phi_0/2$ vortex is shown as the lower surface for comparison.

This is accomplished by choosing the three constants $u_{0i}>0$; see Eqs. (42). Therefore, in this case we must take the plus sign in the three Eqs. (41) as well as in all terms of the energy sum (43). This yields

$$\frac{\epsilon(5\phi_0/2)}{\epsilon_1}=\frac{3}{2}\left(1+\sqrt{\frac{3}{2}}\right). \tag{46}$$

For $m=4$ the total flux would have been $9\phi_0/2$. This, however, is impossible because each arm may contain no more than ϕ_0. Thus, $m=0,2$ exhaust all even possibilities. For the same reason, the only odd m permitted is 1, with the total flux $3\phi_0/2$.

The treatment of the latter case is simple for all λ_i's equal: the root of Eq. (37) is $\eta=1$ and the question of sign choices in Eq. (41) does not arise. We obtain $u_{0i}=0$ and

$$\frac{\epsilon(3\phi_0/2)}{\epsilon_1}=\frac{3}{2}, \tag{47}$$

the energy level in the middle between the ground state energy $\epsilon(\phi_0/2)$ and $\epsilon(5\phi_0/2)$.

Less specific combinations of λ_J's that can still be treated analytically, are considered in the Appendix. We turn now to the general situation of different λ_J's. It is clear in view of the above discussion of the interrelation between the fluxes Φ_i and the constants u_{0i} that the ground state with $\Phi=\phi_0/2$ corresponds to the combination $(-,-,-)$ in the energy (43), in which $0<\eta<1$ is a root of the cubic Eq. (35). Doing this numerically, we obtain the ground state energy as a function of γ_2 and γ_3 shown as a lower surface in Fig. 3.

The case of $\Phi=5\phi_0/2$ corresponds to $(+,+,+)$ and can be treated in a similar manner. However, the situation with $\Phi=3\phi_0/2$ is more involved. First, one has to use for η the root of Eq. (37). Then, the flux $\Phi=3\phi_0/2$ can be distributed among the branches in a number of ways. Each one of them corresponds to a certain combination of signs of u_{0i}'s. Clearly, the combinations $(-,-,-)$ and $(+,+,+)$ are excluded because the first would give the total flux $\Phi<3\phi_0/2$ whereas the second corresponds to $\Phi>3\phi_0/2$.

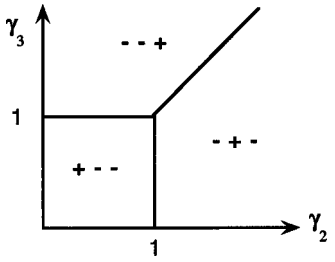

FIG. 4. Domains of parameters $\gamma_2=\lambda_2/\lambda_1, \gamma_3=\lambda_3/\lambda_1$ are shown with sets of signs in the energy sum (43) corresponding to the minimum possible energy of the $3\phi_0/2$ vortex.

We are left with six possibilities: the three having one plus $(+--,\ -+-,\ --,+)$ and another three having one minus $(-++,\ +-+,\ ++-)$; in fact, there are only four combinations to compare, because those which differ only by replacement $\gamma_2 \leftrightarrow \gamma_3$ are physically equivalent. A straightforward comparison of energies (43) for these possibilities shows that for each particular set of $\gamma_{2,3}$ (or of λ_J's), the lowest energy belongs to the set of signs with one plus by the energy term with largest λ_J (or largest among γ_2, γ_3, and 1). This can be interpreted as follows: since the ground state corresponds to the flux $\phi_0/2$ ''attached'' to the intersection, an extra ϕ_0 out of the total $3\phi_0/2$ ''leaks'' into one of the arms. The energy cost of this leakage is minimum for the arm with largest λ_J. Figure 4 shows the domains of $\gamma_{2,3}$ with the sign combinations of the lowest energy.

The energy of the $3\phi_0/2$-vortex vs $\gamma_{2,3}$ (constructed so that in each domain only the lowest possible energy is shown) is plotted as the upper surface in Fig. 3. It is interesting to note that this energy has a maximum of $3\epsilon_1/2$ for $\gamma_2=\gamma_3=1$, which, in fact, is a sharp cusp.

It should be noted that $\epsilon(3\phi_0/2)>\epsilon(\phi_0/2)$ for any $\gamma_{2,3}$; the lower sheet in Fig. 3 is the ground state energy $\epsilon(\phi_0/2)$ shown for comparison. Hence, the state with the flux $3\phi_0/2$ can be considered as an excited state of the tricrystal boundary. This state can decay into the ground state with the flux $\phi_0/2$ by ''emitting'' a ϕ_0-vortex along one of the arms. The decay is possible provided the energy $\epsilon(3\phi_0/2)$ exceeds the combined energy of the ground state, $\epsilon(\phi_0/2)$, and the energy of a vortex at infinity at the arm with largest λ_J, $\epsilon_1/\gamma_{\max}$ ($\gamma_{\max}$ is the largest of $\gamma_2, \gamma_3, 1$). We, therefore, study numerically the quantity

$$\Delta = \frac{\epsilon(3\phi_0/2)}{\epsilon_1} - \frac{\epsilon(\phi_0/2)}{\epsilon_1} - \frac{1}{\gamma_{\max}} \tag{48}$$

as a function of $\gamma_{2,3}$. The result is that Δ is negative in most of the plane γ_2, γ_3 except a relatively narrow region near the cusp at $\gamma_2=\gamma_3=1$. Besides, we found that $|\Delta|<1$. To illustrate this behavior, we plot in Fig. 5 the difference Δ along the line $\gamma_2=\gamma_3$. Along this line, $\Delta>0$ only near $\gamma=1$ (in fact, for $0.94<\gamma<1.24$). One can see that $|\Delta|$ is larger for small γ's than for the large ones. Since this difference characterizes the stability of the state with $3\phi_0/2$, we conclude that the search for this metastable state should be conducted in the domain $\gamma_{2,3}<1$, i.e., in tricrystals with the Josephson length of the π-arm being larger than those of the 0 arms.

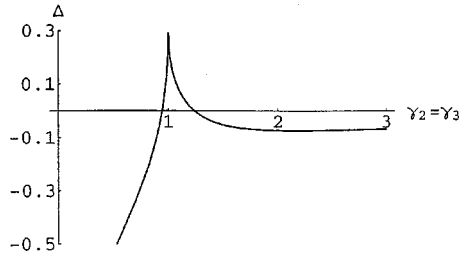

FIG. 5. The energy difference Δ of Eq. (48) between a $3\phi_0/2$ vortex and the combined energy of possible decay products, $\phi_0/2$ at the tricrystal joint and ϕ_0 far away from the joint at the arm with largest Josephson length, in units of ϵ_1 along the line $\gamma_2=\gamma_3$.

IV. DISCUSSION

In scanning superconducting quantum interference device (SQUID) microscopy, vortices with fluxes $3\phi_0/2$ or $5\phi_0/2$ have never been recorded. The discussion above gives a clear reason for this: the corresponding energies are larger than that of $\phi_0/2$. However, we have seen also that the $3\phi_0/2$ vortex can exist as a metastable state because it has a lower energy than the combined energy of $\phi_0/2$ at the intersection and ϕ_0 at infinity. Within the static approach here, the decay process of this metastable state cannot be studied; one would have to solve the time-dependent sine-Gordon equation to see how this transition evolves with time.

It must be noted that the model developed here is constructed for bulk crystals whereas experiments are done on thin films for which the stray fields created by vortices in vacuum contribute substantially to the energy balance. The problem of stability of various configurations of vortices should be addressed separately for a film geometry.

Let us consider a $\phi_0/2$ vortex at the thin film tricrystal joint. The energy of the outside field is approximately $(\phi_0/2\pi)^2/\sqrt{\lambda_L\lambda_J}$ (the magnetostatic self-energy of a ''charge'' $\phi_0/2\pi$ occupying roughly the area $\lambda_L\lambda_J$ of the film). This energy would have been smaller if the flux, instead of extending to infinity, would cross the film and come back to the vortex from under the film. This, however, cannot happen for the flux $\phi_0/2$, unless the film contains another tricrystal with one π arm through which the flux $-\phi_0/2$ can cross the film from the upper to lower half-spaces.

Clearly, this ban does not hold for a vortex $3\phi_0/2$: the part ϕ_0 of this flux can cross the film far from the tricrystal intersection creating a Josephson vortex of $-\phi_0$ at one of the arms. The antivortex, $-\phi_0$, is attracted to the vortex $3\phi_0/2$ that may lead to annihilation of $-\phi_0$ and reduction of $3\phi_0/2$ to $\phi_0/2$. The energy requirement for this process to occur is

$$\epsilon(3/2,0)d+\varepsilon(3/2,0)>\epsilon(1/2,0)d+\varepsilon(1/2,0)+\epsilon(1,\infty)d + \varepsilon(1,\infty). \tag{49}$$

Here, ε is the energy of the stray fields, the first argument is the flux in units of ϕ_0, and the second labels positions; d is the film thickness (the energies in the main text were calculated per unit length in the field direction). One can check that for all λ_J's equal, this inequality is satisfied (it holds separately for both the Josephson and the stray parts of the energy). However, as we have seen above, the case of equal

λ_J's corresponds to the maximum energy of the $3\phi_0/2$ vortex. For a general case the inequality (49) reads

$$d\epsilon_1\Delta > \varepsilon(1/2)+\varepsilon(1)-\varepsilon(3/2). \tag{50}$$

This translates to $d/\sqrt{\lambda_L\lambda_J} < \pi/|\Delta|$ with λ_J as an average Josephson length. Since $|\Delta|<1$ (see Fig. 5), this condition is satisfied for thin enough films. Therefore, we do not expect the $3\phi_0/2$ vortex to be observable if

$$d < \sqrt{\lambda_L\lambda_J}. \tag{51}$$

In experiments of Ref. 3, $d\approx 0.12\,\mu$, $\lambda_L \approx 0.15\,\mu$, and $\lambda_J \approx 4\,\mu$, so that the decay condition for the $3\phi_0/2$ vortex is well satisfied. In thicker films, however, this condition might be violated and the $3\phi_0/2$ state may become stable as is the case in the bulk. Note, however, that it may be difficult to grow cuprate films on $SrTiO_3$ substrates epitaxially as thick as $0.5\,\mu$m, which would be required to test these ideas in tricrystal experiments.

A similar analysis of the state carrying $5\phi_0/2$ shows that for arbitrary λ_J's the Josephson energy of this state obeys $\epsilon(5/2,0) > \epsilon(3/2,0)+\epsilon(1,\infty)$ and the same inequality holds for magnetic fields in vacuum: $\varepsilon(5/2) > \varepsilon(3/2)+\varepsilon(1)$. In other words, both Josephson and stray field energies favor the $3\phi_0/2$ vortex at the tricrystal intersection and a ϕ_0 far away from the joint to a $5\phi_0/2$ vortex at the joint.

We conclude noting that the static properties of the tricrystal Josephson boundaries discussed here do not exhaust the rich physics of these systems. We have shown that for the three conventional tricrystal arms, the restriction (18) should be satisfied for a ϕ_0 vortex to be in equilibrium at or near the intersection. If the largest Josephson length exceeds the sum of the other two, the tricrystal ceases to be a potential well. Tricrystal substrates with all 0-junctions have been fabricated and studied in symmetry tests using ring geometries.[11,12] Some of the predictions made in this paper can be tested by growing epitaxial unpatterned films of the cuprate superconductors on these substrates.

If one of the tricrystal arms is a π junction, a $\phi_0/2$ vortex at the intersection exists in the ground state, whereas $3\phi_0/2$ and $5\phi_0/2$ correspond to possible but, in general, metastable states. For certain combinations of Josephson lengths, the $3\phi_0/2$ state has lower energy than the combined energy of the $\phi_0/2$ vortex at the tricrystal joint and a ϕ_0 vortex far from the intersection. Conditions are discussed under which the $3\phi_0/2$ vortex can be observed. A very interesting question of dynamic behavior of tricrystal Josephson boundaries is still to be addressed.

ACKNOWLEDGMENTS

We use this opportunity to thank K. Moler for many illuminating discussions. Ames Laboratory is operated for the U. S. Department of Energy by Iowa State University under Contract No. W-7405-Eng-82. The work at Ames was supported by the Office of Basic Energy Sciences.

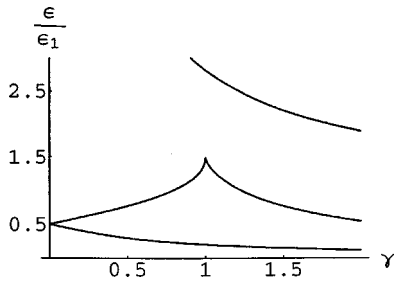

FIG. 6. Energies of the states carrying fluxes (from the bottom up) $\phi_0/2$, $3\phi_0/2$, and $5\phi_0/2$ in units of ϵ_1 for $\gamma_2=\gamma_3=\gamma$.

APPENDIX

If the two 0-arms are the same, $\gamma_2=\gamma_3=\gamma$, the cubic equation (35) has a root

$$\eta = \frac{\sqrt{1+8\gamma^2}-1}{4\gamma^2} < 1. \tag{A1}$$

We substitute this in Eq. (43) with the set of signs $(-,-,-)$ to obtain the energy $\epsilon(\phi_0/2)$; the combination $(+,+,+)$ gives $\epsilon(5\phi_0/2)$. These energies *versus* γ are plotted in Fig. 6 as the bottom and top curves.

For $\Phi=3\phi_0/2$, the cubic equation (37) has two positive roots:

$$\eta_1=1, \quad \eta_2=\frac{\sqrt{1+8\gamma^2}+1}{4\gamma^2}. \tag{A2}$$

One can see that for $\gamma<1$, the second root exceeds 1, and therefore, $\eta_1=1$ is the only root acceptable. According to Fig. 4 we choose the signs $(+,-,-)$ in the energy (43) and obtain

$$\frac{\epsilon(3/2)}{\epsilon_1} = \frac{1}{2}\left(1+2\frac{1-\sqrt{1-\gamma^2}}{\gamma}\right), \quad \gamma<1. \tag{A3}$$

If $\gamma>1$, one can see that $\eta_2<1$. Using this root and either $(-,+,-)$ or $(-,-,+)$ as the sign combination, we obtain

$$\frac{\epsilon(3/2)}{\epsilon_1} = \frac{1}{2}\left(1+\frac{2}{\gamma}-\sqrt{1-\eta_2^2}\right), \quad \gamma>1. \tag{A4}$$

When $\gamma\to 1$, the energies (A3) and (A4) tend to 3/2 as they should; see Eq. (47). Formally, however, $\gamma=1$ is a singular point: the derivatives $d\epsilon/d\gamma$ are divergent at both sides of this point. Physically, this means that the state with equal fluxes on the arms ($\Phi_i=\phi_0/2$ correspond to $\gamma=1$) is unstable with respect to small deviations from equal λ_J. The energy $\epsilon(3/2)$ is plotted in Fig. 6 along with $\epsilon(1/2)$ and $\epsilon(5/2)$ *versus* γ.

If the λ_J of one of the 0 arms is the same as the λ_J of the π arm (e.g., $\gamma_2=1$), one of the $\pm 1/\gamma_3$ is a root of the cubic Eqs. (35) and (37), and the rest of the roots are readily found. We will not go into details of this case since physically it brings nothing new.

[1] C.C. Tsuei, J.R. Kirtley, C.C. Chi, L.S. Yu-Janes, A. Gupta, T. Shaw, J.Z. Sun, and M.B. Ketchen, Phys. Rev. Lett. **73**, 593 (1994).

[2] J.H. Miller, Jr., Q.Y. Ying, Z.G. Zou, N.Q. Fan, J.H. Xu, M.F. Davis, and J.C. Wolfe, Phys. Rev. Lett. **74**, 2347 (1995).

[3] J.R. Kirtley, C.C. Tsuei, M. Rupp, J.Z. Sun, Lock See Yu-Jahnes, A. Gupta, M.B. Ketchen, K.A. Moler, and M. Bhushan, Phys. Rev. Lett. **76**, 1336 (1996).

[4] M. Sigrist and T.M. Rice, J. Phys. Soc. Jpn. **61**, 4283 (1992); Rev. Mod. Phys. **67**, 503 (1995).

[5] L.N. Bulaevskii, V.V. Kuzii, and A.A. Sobyanin, Pis'ma Zh. Éksp. Teor. Fiz. **25**, 314 (1977) [JETP Lett. **25**, 290 (1977)].

[6] Z. Radović, M. Ledvij, L. Dobrosavljević-Grujić, A.I. Buzdin, and J.R. Clem, Phys. Rev. B **44**, 759 (1991).

[7] I.O. Kulik and I.K. Yanson, *The Josephson Effect in Superconductive Tunneling Structures* (Israel Program for Scientific Translation, Jerusalem, 1972).

[8] A. Barone and G. Paterno, *Physics and Applications of the Josephson Effect* (Wiley, New York, 1982).

[9] J.R. Kirtley, K.A. Moler, and D.J. Scalapino, Phys. Rev. B **56**, 886 (1997).

[10] J.H. Xu, J.H. Miller, Jr., and C.S. Ting, Phys. Rev. B **51**, 11 958 (1995).

[11] J.R. Kirtley, C.C. Tsuei, J.Z. Sun, C.C. Chi, Lock See Yu-Jahnes, A. Gupta, M. Rupp, and M.B. Ketchen, Nature (London) **373**, 225 (1995).

[12] C.C. Tsuei and J.R. Kirtley, Physica C **282-287**, 4 (1997).